Available online at www.sciencedirect.com
SCIENCE DIRECT
Journal of the European Ceramic Society 26 (2006) 703–710
www.elsevier.com/locate/jeurceramsoc

Thermal properties of silicon carbide composites fabricated with chopped Tyranno® Si–Al–C fibres

Kiyoshi Itatani [a,*], Tsuyoshi Tanaka [a], Ian J. Davies [b]

[a] *Department of Chemistry, Faculty of Science and Engineering, Sophia University, 7-1 Kioi-cho, Chiyoda-ku, Tokyo 102-8554, Japan*
[b] *Department of Mechanical Engineering, Curtin University of Technology, G.P.O. Box U1987, Perth, WA 6845, Australia*

Available online 15 August 2005

Abstract

Thermal diffusivity, a, and thermal conductivity, κ, between room temperature and 600 K were investigated for SiC composites containing 0–50 mass% of Tyranno® Si–Al–C (SA) fibre (mean length: 394 μm) hot-pressed at 1800 °C for 30 min under a pressure of 31 MPa. The monolithic SiC specimen possessed κ of 32.1 W m^{-1} K^{-1} at room temperature; no significant changes were found for the SiC composite containing ≤20 mass% of SA fibre addition. However, further increases in the amount of SA fibre to 50 mass% improved κ to a maximum of 56.3 W m^{-1} K^{-1}. The value of a for the SiC composite containing 40 mass% of SA fibre was 0.185 cm^2 s^{-1} at room temperature and decreased to 0.120 cm^2 s^{-1} at 600 K. In addition, SiC composites using 40 mass% of SA fibre with a carbon interface of approximately 100 nm were fabricated. The effect of this interface on a and κ was marginal.

Keywords: Hot pressing; Composites; Thermal properties; Thermal conductivity; SiC

1. Introduction

Monolithic silicon carbide (SiC) ceramic possesses several important characteristics, including excellent chemical and wear resistance, high hardness, and high thermal conductivity, that have favoured its use under severe environmental conditions. Despite these advantages, the relatively poor fracture toughness of monolithic SiC, e.g., 2.4 MPa m$^{1/2}$,[1] has limited its scope for many structural applications. One method to increase the fracture toughness of SiC is to incorporate a reinforcement phase that promotes crack deflection at the interface. For example, fracture toughness values of up to 40 MPa m$^{1/2}$ have been reported[2] for continuous fibre-reinforced (CFR) SiC composites containing 3-D woven Tyranno® Si–Ti–C–O fibres.

Whilst CFR-SiC composites are known to exhibit excellent mechanical properties under a variety of test conditions,[3] the most common manufacturing techniques, namely chemical vapour infiltration (CVI)[4] and polymer impregnation and pyrolysis (PIP),[5] have disadvantages including processing times on the order of weeks or months, high cost, and relatively high residual porosity (typically > 5%). In contrast to this, discontinuous fibre-reinforced (DFR) SiC composites are significantly cheaper to produce and also possess enhanced mechanical properties,[6–9] albeit not to the same extent as for CFR-SiC composites. Whilst work on DFR-SiC composites was originally concerned with amorphous fibres, e.g., Tyranno® Si–Ti–C–O,[10] these fibres are susceptible to thermal decomposition and crystallite growth at elevated temperature, resulting in reduced mechanical performance. However, recently developed near-stoichiometric Tyranno® Si–Al–C (SA) fibre is able to maintain a tensile strength of >2.5 GPa in inert and air atmospheres up to 1900 and 1000 °C, respectively.[11]

In light of this, the present authors have investigated[12] the mechanical properties of hot-pressed SiC composites containing SA fibre (mean length: 394 μm), and found the fracture toughness to reach a maximum of 4.0 MPa m$^{1/2}$ for a SiC composite containing 30 mass% of SA fibre and 5.8 MPa m$^{1/2}$ for a SiC composite containing SA fibres with a carbon interface (thickness: approximately 100 nm). In addition, an

* Corresponding author. Tel.: +81 3 3238 3373; fax: +81 3 3238 3361.
E-mail address: itatani@sophia.ac.jp (K. Itatani).

0955-2219/$ – see front matter © 2005 Elsevier Ltd. All rights reserved.
doi:10.1016/j.jeurceramsoc.2005.07.008

investigation on the effect of mean fibre length[13] resulted in a fracture toughness of 6.0 MPa $m^{1/2}$ being achieved for a composite containing 40 mass% of SA fibre (mean length: 706 μm) with a carbon interface; this value is believed to be the highest so far achieved for DFR-SiC composites.

In addition to superior mechanical properties, CFR- and DFR-SiC composites are often required to possess a high thermal conductivity, κ, in order to reduce mechanical stresses that arise due to the presence of thermal gradients within the component. For example, the thermal shock resistance of any brittle material can be characterised by the classical parameter, R', with[14]:

$$R' = \kappa \frac{\sigma}{\alpha E}(1-\nu) \quad (1)$$

where σ is the strength, α is the coefficient of thermal expansion, E is Young's modulus, and ν is Poisson's ratio.

The values of κ for single-crystal SiC[15] and polycrystalline SiC[16] are 490 and (up to) 270 W m^{-1} K^{-1}, respectively. In contrast to this, values of κ for CFR-SiC composites measured in the transverse direction are often <20 W m^{-1} K^{-1} at room temperature, although values as high as 75 W m^{-1} K^{-1} have been reported as shown in Table 1.[17–22] The value of κ for composite materials is known to depend on the individual values of the fibre, κ_f, matrix, κ_m, and interface layer, κ_i, together with the processing parameters and amount and morphology of any porosity.[20,23–26] Several approaches have been taken towards predicting the value of κ for composite materials with the simplest methods being the parallel and series models as follows:

$$\kappa = V_f \kappa_f + (1 - V_f)\kappa_m \quad (2)$$

$$\frac{1}{\kappa} = \frac{V_f}{\kappa_f} + \frac{(1-V_f)}{\kappa_m} \quad (3)$$

where V_f is the volume fraction of fibres. A more sophisticated approach is that derived by Kingery et al.[27] and based on the Maxwell-Eucken equation[28] with the assumption that the fibres are well dispersed and not touching one another:

$$\kappa = \kappa_m \left\{ \frac{1 + 2V_f((1-\kappa_m/\kappa_f)/2(\kappa_m/\kappa_f)+1)}{1 - V_f((1-\kappa_m/\kappa_f)/(\kappa_m/\kappa_f+1))} \right\} \quad (4)$$

Whilst κ has been determined for ceramic matrix composites reinforced with SiC powder or whiskers,[23,29–31] there is a relative dearth of data available concerning the range of κ values expected within DFR-SiC composites.[7] The present work is thus concerned with an investigation on the thermal properties of a SiC composite containing chopped SA fibre, whose manufacture and resulting mechanical properties have been the subject of previous work by the authors.[12,13]

2. Experimental procedure

2.1. Fabrication of the SiC composite containing SA fibre

Hot-pressed compacts in this work utilised ultrafine SiC powder obtained via the pyrolysis of triethylsilane ($(C_2H_5)_3SiH$: AZmax Co. Ltd., Ichihara, Japan) in argon at 1100 °C, using a chemical vapour deposition (CVD) technique. The resulting SiC powder (specific surface area (SSA): 53.4 m^2 g^{-1}; mean particle size: 43 nm) was further heated in air at 500 °C for 2 h in order to eliminate any residual carbon. In addition, aluminium carbide (Al_4C_3) was utilised as a sintering aid and prepared from the pyrolysis

Table 1
Transverse thermal conductivity (TC) of various continuous fibre-reinforced SiC composites at room temperature (RT) and elevated temperature

Component		Fibre configuration	Porosity (%)	Temperature (°C)	TC (W mi^{-1} K^{-1})	References
Fibre	Matrix					
Nicalon®	SiC (CVI)	3-D woven	10	RT 800	11.5–12.5 6.5–7.5	Giancarli et al.[17]
CVR of SiC[a]	SiC (CVR)	1-D	15	RT 1000	75 35	Kowbel et al.[18]
Hi-Nicalon®	Si—C—O[b]	2-D woven	Not available	RT 1000	5–11 5–15	Yoshida et al.[19]
Hi-Nicalon®	SiC (CVI)	2-D woven	6–10	RT 1000	13 9	Youngblood et al.[20]
Tyranno® SA	SiC (NITE)	2-D woven	3–6	RT 1000	17–29 15–20	Katoh et al.[21]
Tyranno® SA	SiC (CVI)	3-D woven	<10	RT 1000	40–50 24	Yamada et al.[22]
Hi-Nicalon® Type S	*SiC(CVI)*	3-D woven	<10	RT 1000	36 20	Yamada et al.[22]

CVI: chemical vapour infiltration; CVR: chemical vapour reaction; NITE: nano-infiltration and transient eutectic-phase.
[a] SiC was obtained from Toray® T-300 carbon fibre.
[b] Si—C—O was derived from polycarbosilane.

of trimethylaluminum ($(CH_3)_3Al$: Nippon Aluminum Alkyls Ltd., Tokyo, Japan) in argon at 1100 °C using a CVD technique; the SSA and mean particle size were 58.0 $m^2\ g^{-1}$ and 39 nm, respectively.

The required amount of SiC powder was first mixed with 5 mol% of Al_4C_3 powder[7] in the presence of hexane using an alumina mortar and pestle. Following this, the powder was mixed with 0–50 mass% of SA fibre (Ube Industries, Ltd., Ube City, Japan) that had been ultrasonically dispersed in the presence of hexane and then dried in air. Approximately, 1.5 g of the mixture was first uniaxially pressed at 50 MPa and then isostatically pressed at 100 MPa to form a disk with a diameter of 20 mm and a thickness of 2 mm. Finally, the disk was hot-pressed at 1800 °C for 30 min under a uniaxial pressure of 31 MPa in an argon atmosphere.[6]

Two types of SA fibre were used in the present work. As shown in the SEM micrographs (Fig. 1), the standard SA fibre possessed fibre diameters in the range of 5–10 μm and length distributions in the range of 200–600 μm (Fig. 1a); the mean length and diameter of the SA fibres were 394 and 7.5 μm, respectively. The higher magnification SEM micrograph of the standard SA fibre (Fig. 1b) indicated the surface to be essentially smooth, whilst that of the SA fibre with a carbon interface (SA/C) obtained by treatment in a CO atmosphere at 1700 °C for 1 h was relatively rough in nature (Fig. 1c). According to the Auger depth profiles for the SA/C fibre (data provided by Ube Industries Ltd.), the carbon interface thickness was estimated to be 100 nm.

2.2. Characterisation

The relative density of hot-pressed compact was calculated by dividing the bulk density by the true density. The bulk density was measured on the basis of mass and dimensions, whilst true density was measured picnometrically at 25.0 °C using *n*-hexane as a replacement liquid after the hot-pressed compact was pulverized using a zirconia mortar and pestle. Crystalline phases within the hot-pressed compact were examined using an X-ray diffractometer (XRD; Model RINT2100V/P, Rigaku, Tokyo, Japan; 40 kV, 40 mA) and monochromatic CuKα radiation. The microstructure of the hot-pressed compact was analysed using a field-emission scanning electron microscope (FE-SEM; Model S-4500, Hitachi, Tokyo, Japan), following coating of the surface with Pt–Pd using an ion coater (Model E-1030, Hitachi, Tokyo, Japan) in order to avoid charging effects; some of the hot-pressed compacts were etched using Murakami's reagent (10 g of NaOH and 10 g of $K_3Fe(CN)_6$ in 40 cm^3 H_2O at 110 °C for 20–30 min), after polishing the surfaces of compacts.

Thermal properties of compacts in the direction parallel to hot pressing, i.e., transverse direction, were investigated using either laser-flash or photo-flash techniques; plate-like specimens with dimensions of approximately 10 mm × 10 mm × 1 mm were used for the laser flash technique (Model TC-7000, Ulvac-Riko, Yokohama, Japan) at room temperature, whereas cylindrical specimens with

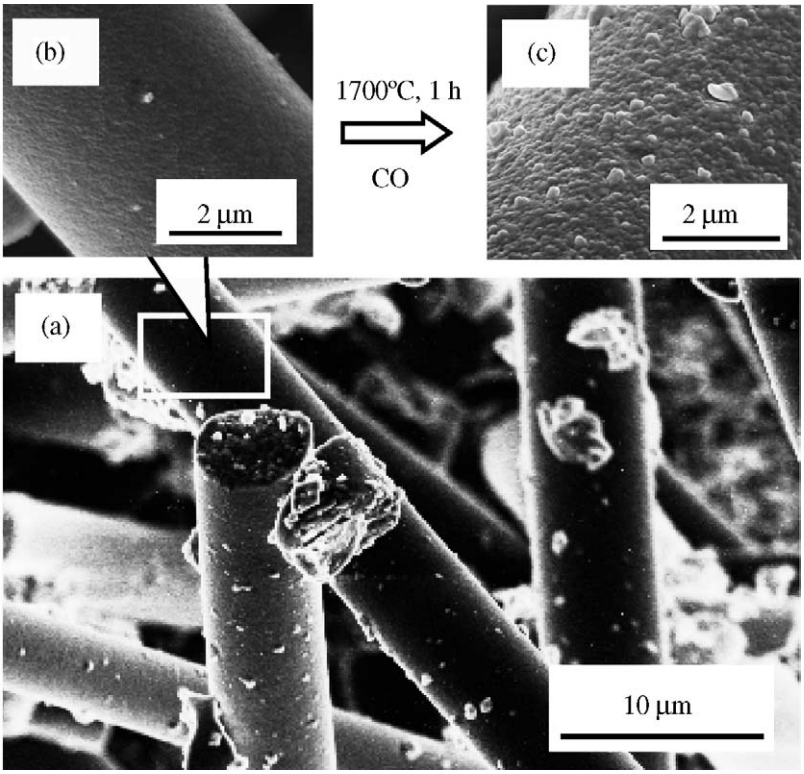

Fig. 1. SEM micrographs of the chopped SA fibre. (a) Overview; (b) Surface of SA fibre; (c) SA fibre with a carbon interface.

diameter and thickness of 20 and 1 mm, respectively, were used for the photo-flash technique (Compotherm Messtechnik GmbH, Syke, Germany) between room temperature and 600 K. These specimens were polished to a 0.5 μm finish, prior to being coated with a thin layer of gold and then carbon in order to aid energy absorption and transfer to the specimen. The experimental accuracy of the thermal conductivity measurements was estimated to be within ±5%. The thermal conductivity of each specimen was calculated from the thermal diffusivity data, using the following equation[32]:

$$\kappa = a\rho C_v \tag{5}$$

where a is the thermal diffusivity, ρ is the density, and C_v is the heat capacity at constant volume. Values for C_v of 0.73 (SiC matrix)[33] and 0.669 J g^{-1} K^{-1} (SA fibre)[34] were used in the present work with C_v for specimens being calculated according to the respective proportions of the components. It is known that the value of κ in SiC composites is strongly dependent on the level of porosity.[19] One relationship that has been used to take into account this factor is[35]:

$$\kappa_{\text{Exp}} = \kappa_{\text{Ideal}} \left(\frac{1 - P}{1 + 11P^2} \right) \tag{6}$$

where κ_{Exp} is the value of κ for the composite containing porosity, κ_{Ideal} is the value of κ for a composite containing no porosity, and P is the fractional porosity. Unless otherwise stated, all values of κ mentioned in this work were corrected using Eq. (6) in order to obtain the intrinsic (i.e., κ_{Ideal}) value; this correction increased κ by an average of 7% for the materials under investigation.

3. Results and discussion

3.1. Relative density, phase composition and microstructure anisotropy

The effect of processing parameters on the relative density (i.e., bulk density/true density) and mechanical properties of these composites has been discussed in detail elsewhere[12,13]; it is noted here that the relative density exceeded 95% for all specimens. The amount and position of the porosity were found to depend on the amount of SA fibre. For example, the SiC composite containing 50 mass% of SA fibre tended to possess the majority of its porosity within the fibre agglomerates.[12] The crystalline phases of the composites were examined using XRD with a typical result being shown in Fig. 2. All of the composites were comprised of mainly α- and β-SiC, together with a small amount of α-Al_2O_3. The presence of α-Al_2O_3 is derived from the reaction of Al_4C_3 with atmospheric moisture[36] and/or that of Al_4C_3 with the layer of SiO_2 often found on the surface of SiC particles.[37,38]

The use of uniaxial pressure during powder compaction and hot pressing was expected to significantly influence the arrangement of chopped SA fibres within the SiC composite. Typical SEM micrographs of etched surfaces parallel and perpendicular to the direction of loading are shown in Fig. 3. The SA fibres were found to be preferentially aligned perpendicular to the direction of uniaxial loading. The preferential alignment of SA fibres in the SiC matrix is thought to have originally occurred during uniaxial pressing of the powder mixture; the alignment of fibres may have been further promoted due to uniaxial pressing during hot pressing.

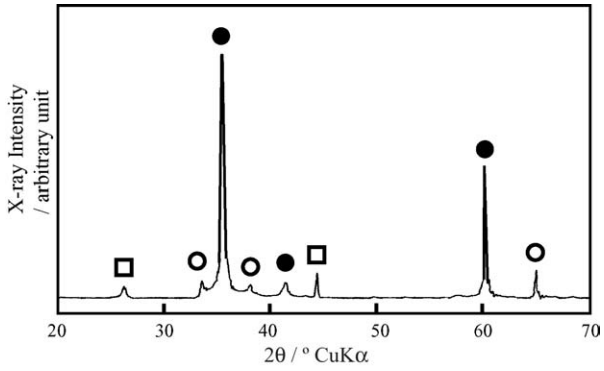

Fig. 2. Typical XRD pattern of a SiC composite containing 40 mass% of SA fibre hot-pressed at 1800 °C for 30 min under a pressure of 31 MPa. (○) α-SiC; (●) β-SiC; (□) α-Al_2O_3.

3.2. Effect of chopped SA fibre amount with and without carbon interface on the thermal conductivity at room temperature

As shown in Fig. 3, the preferential alignment of SA fibres in the SiC matrix should also exhibit anisotropic thermal behaviour. In the present work, however, only the thermal properties parallel to the direction of loading, i.e., transverse direction, have been considered due to (i) the difficulty in preparing a specimen of sufficient thickness to test in the direction perpendicular to loading, and (ii) previous research having tended to concentrate on thermal properties in the transverse direction,[19,20] as this is the limiting factor in many applications, e.g., fusion power blankets.[39]

Thermal conductivity data in the transverse direction has been shown in Fig. 4, together with estimates for the theoretical thermal conductivities according to Eqs. (2)–(4). The porosity-corrected value of κ for the monolithic SiC specimen (32.1 W m^{-1} K^{-1}) was used for κ_m with a value of 64.6 W m^{-1} K^{-1} being assumed for κ_f [40]. Regarding the experimental data, the addition of up to 20 mass% of SA fibre produced no increase in κ; however, a further increase in SA fibre amount to 30 mass% led to a significant increase in κ to 43.4 W m^{-1} K^{-1}. The maximum κ value achieved for the SiC composite containing SA fibres was 56.3 W m^{-1} K^{-1} for the case of 50 mass% of SA fibre.

Whilst the general trend of increasing κ with increasing V_f was consistent between the experimental data and predicted values from the different models, the predicted values were all overestimated for SiC composites containing 10–20 mass%

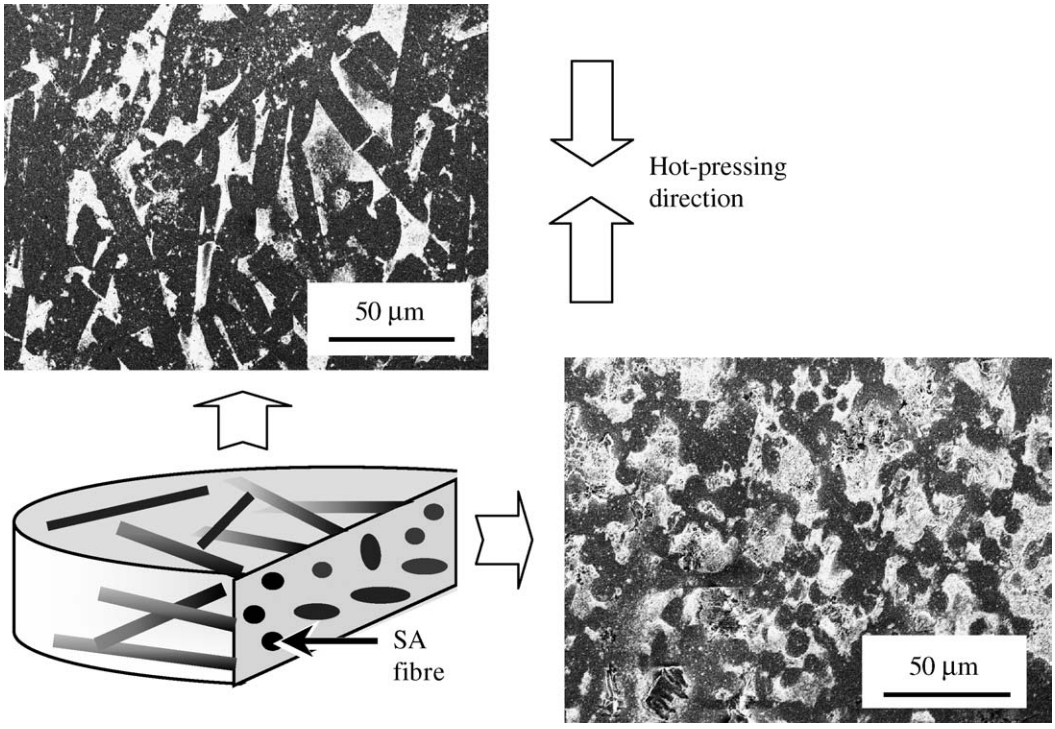

Fig. 3. Schematic diagram of the hot pressing configuration, together with typical SEM micrographs of the surface perpendicular and parallel to the direction of loading for a SiC composite containing 30 mass% of SA fibre hot-pressed at 1800 °C for 30 min under a pressure of 31 MPa.

of SA fibre and underestimated for the SiC composite containing 50 mass% of SA fibre. The relatively low κ value for the monolithic SiC specimen is attributed to (i) significant phonon scattering at grain boundaries where a large number of defects are present, and (ii) the presence of small grains. Whilst the value of κ for the composite would have been expected to increase with the addition of up to 20 mass% of SA fibre (due to $\kappa_f > \kappa_m$), one explanation for the actual trend would be the change in pore geometry for composites containing small additions of fibre. A further increase in SA fibre amount to 40 mass% led to an increase in κ to 40.5 W m^{-1} K^{-1}, which is attributed to the decrease in porosity. The maximum κ value achieved for the SiC composite containing 50 mass% of SA fibre, 56.3 W m^{-1} K^{-1}, is higher than that achieved for most of the CFR-SiC composites shown in Table 1. This phenomenon may be explained in terms of the percolation threshold[41] being passed, i.e., the fibres forming a continuous network throughout the specimen.

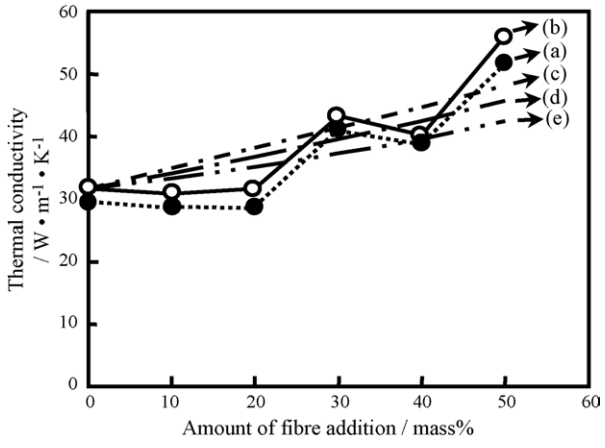

Fig. 4. Effect of SA fibre amount on the thermal conductivity (room temperature) for a SiC composite hot-pressed at 1800 °C for 30 min under a pressure of 31 MPa. (a) Present data; (b) present data corrected for porosity; (c) theory (two-phase parallel); (d) theory (two-phase serial); (e) theory (Maxell-Eucken).

In previous work by the authors it was found that utilising SA fibres with a carbon interface led to a significant increase in mechanical properties.[12,13] In order to determine any similar effect on the thermal properties, a SiC composite was fabricated using 40 mass% of SA/C fibre. The results of this comparison are shown in Fig. 5. For both a and κ, the addition of 40 mass% of either SA or SA/C fibre produced a significant increase in a and κ on the order of 30–40% compared to the case of the monolithic SiC specimen; however, there was only a marginal difference in values between these two composites. The influence of interfaces on the thermal conductivity of SiC composites was first investigated by Hasselman and Johnson[42] with recent work focussing on SiC composites in particular.[20,43] The similarity of the results for the composites with and without the carbon layer is consistent with that predicted for SiC composites containing thin interface layers with high thermal conductivity.[43] Moreover, from consideration of the thickness of the carbon layer, the total volume fraction of the carbon layer was estimated to be less than 3%.

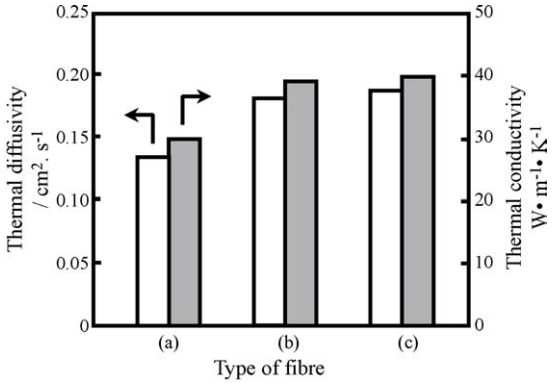

Fig. 5. Effect of SA fibre addition and fibre type on the thermal diffusivity (room temperature) and thermal conductivity for a SiC composite hot-pressed at 1800 °C for 30 min under a pressure of 31 MPa. (a) Monolithic SiC specimen; (b) SiC composite containing 40 mass% of SA fibre; (c) SiC composite containing 40 mass% of SA/C fibre.

Taken together, these facts suggest that the effect of a carbon interface on κ may be marginal.

3.3. Effect of chopped SA fibre amount with and without carbon interface on the thermal conductivity at elevated temperature

The effect of test temperature (295–600 K) on thermal diffusivity was determined for the cases of the monolithic SiC specimen and the SiC composites containing 40 mass% of SA and SA/C fibres. The results are shown in Fig. 6. Whilst the value of a for the monolithic SiC specimen was $0.134\,cm^2\,s^{-1}$ at room temperature, this decreased gradually to reach $0.091\,cm^2\,s^{-1}$ at 600 K. The trends in a for both composites were similar with an initial value of $0.18\,cm^2\,s^{-1}$ decreasing to 0.11–0.12 $cm^2\,s^{-1}$ at 560–580 K. The temperature dependence of a for both composites was similar and both greater than that of the monolithic SiC specimen.

If the heat transport within the material is mainly due to lattice vibrations (i.e., phonon conduction) then a can be given by[44]:

$$a = \frac{1}{3} v_s l_{tot} \tag{7}$$

where v_s is the mean phonon velocity and l_{tot} is the total mean free path of the phonons. It has been shown that l_{tot} is dominated by extrinsic scattering events (i.e., defects and grain boundaries) at low temperature and phonon–phonon scattering at high temperature. Recent work by Bruls[45] and Bruls et al.[46] has indicated that the temperature dependence of a can be closely approximated by the following relationship:

$$a^{-1} = A'T + B' \qquad \text{for } T > \frac{\tilde{\theta}}{b} \tag{8}$$

with

$$\tilde{\theta} = \frac{\theta}{n^{1/3}} \tag{9}$$

where T is the temperature, $\tilde{\theta}$ is the reduced Debye temperature[47], b is a constant ($\approx$2)[44], θ is the Debye temperature (1.2×10^3 K for SiC)[48], and n is the number of atoms per primitive unit cell (4–12 for SiC depending on the polytype).[49] The above equations indicate the temperature dependence to be valid in SiC for temperatures above $\theta/bn^{1/3}$, i.e., 262–378 K depending on the polytype, which validates the present investigation. Whilst the magnitude of A' is solely determined by intrinsic lattice characteristics, that of B' is determined, in addition to the intrinsic lattice characteristics, by the presence of impurities and microstructure.[45]

In order to apply the above theory, the present data was converted to a^{-1} versus T coordinates and fitted with a straight line, as shown in Fig. 7. The slope of

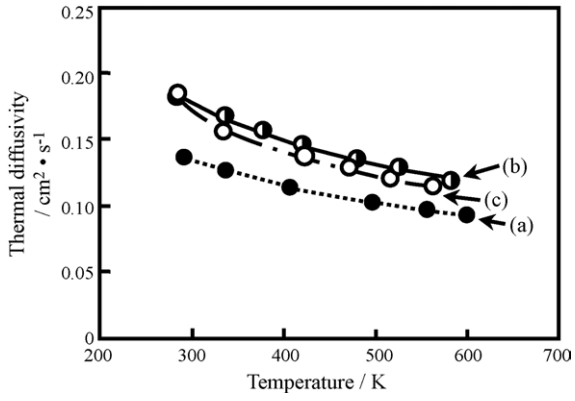

Fig. 6. Effect of SA and SA/C fibre addition on the temperature dependence of thermal diffusivity for a SiC composite hot-pressed at 1800 °C for 30 min under a pressure of 31 MPa. (a) Monolithic SiC specimen; (b) SiC composite containing 40 mass% of SA fibre; (c) SiC composite containing 40 mass% of SA/C fibre.

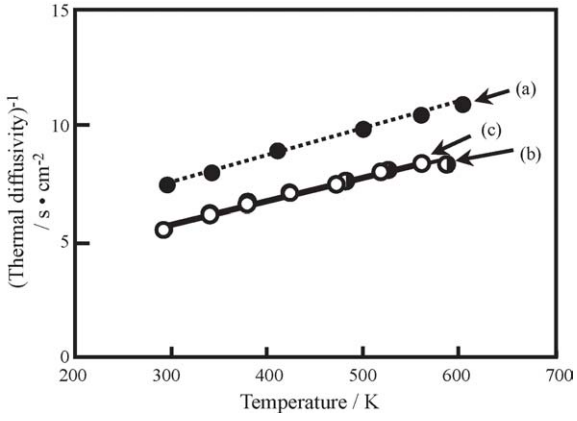

Fig. 7. Effect of SA and SA/C fibre addition on the temperature dependence of reciprocal thermal diffusivity for a SiC composite hot-pressed at 1800 °C for 30 min under a pressure of 31 MPa. (a) Monolithic SiC specimen ($a^{-1} = 1.14 \times 10^{-3}\,T + 4.13$); (b) SiC composite containing 40 mass% of SA fibre ($a^{-1} = 0.97 \times 10^{-2}\,T + 2.74$); (c) SiC composite containing 40 mass% of SA/C fibre ($a^{-1} = 1.12 \times 10^{-2}\,T + 2.26$).

the straight line, i.e., A' in Eq. (8), was in a range of $0.97–1.14 \times 10^{-2}\,cm^{-2}\,s\,K^{-1}$. The slope was similar for each of the composites and specimens within an experimental accuracy of ±20%.[45,46] As mentioned earlier, the value of A' is determined by the intrinsic lattice characteristics and thus, with the matrix being essentially identical for each of the composites and specimens, it was not surprising that the values of A' should be similar. One possible explanation for the slight difference in A' between specimens might be the presence of reactions between the fibre surface, SiC and Al_4C_3 matrix components during hot pressing.

In contrast to the similarity in A' values, the value of B' was significantly different for the monolithic SiC specimen ($B' = 4.13\,s\,cm^{-2}$), compared to that of the SiC composites containing 40 mass% of fibre, i.e., $B' = 2.74\,s\,cm^{-2}$ for the case of SA fibre addition and $2.26\,s\,cm^{-2}$ for the case of SA/C fibre addition. As mentioned previously, the value of B' is determined by the presence of impurities and the microstructure (in addition to the intrinsic lattice characteristics),[45] so that large differences might naturally be expected between the monolithic specimen and composites. The present investigation has thus shown the A' and B' parameters to be able to easily distinguish between a monolithic SiC specimen and DFR-SiC composites and yet be sensitive to the underlying similarities in the matrix components.

4. Conclusions

The transverse thermal conductivity, κ, and thermal diffusivity, a, between room temperature and 600 K was investigated for a discontinuous fibre-reinforced SiC/SiC composite containing 0–50 mass% of chopped Tyranno® Si–Al–C (SA) fibre with a mean length of 394 μm. The composites had been manufactured using the uniaxial hot-pressing method (1800 °C/30 min/31 MPa) and utilised nano-sized silicon carbide (SiC) powder for the matrix, together with 5 mol% of aluminium carbide (Al_4C_3) as a sintering aid; the relative densities being >95% for all specimens. The main conclusions of this work were that:

(i) The value of κ was $32.1\,W\,m^{-1}\,K^{-1}$ for the monolithic SiC with almost no change for composites containing 20 mass% of SA fibre. However, further increases in fibre content resulted in a maximum of $56.3\,W\,m^{-1}\,K^{-1}$ for the composite containing 50 mass% of fibre.

(ii) The influence of carbon interface (~100 nm) on the fibre, SA/C, was investigated for a composite containing 40 mass% of fibre. Compared to the composite containing standard SA fibre, the composite containing SA/C fibre showed only a marginal increase in κ and a and it was concluded that the use of fibres with a carbon interface had negligible effect on the thermal properties.

(iii) The effect of temperature on a was investigated with the relationship being similar for the composites containing 40 mass% of SA and SA/C fibre with a room temperature value of $\sim 0.185\,cm^2\,s^{-1}$ decreasing to a value of $\sim 0.120\,cm^2\,s^{-1}$ at 600 K; these values being significantly higher compared to that of the monolithic SiC.

(iv) Calculation of the A' and B' parameters noted by Bruls et al. indicated the A' values to be similar ($0.97–1.14 \times 10^{-2}\,cm^{-2}\,s\,K^{-1}$) for the composites and monolithic SiC whilst the B' values were similar for the composites (2.74 and $2.26\,s\,cm^{-2}$) but different from that of the monolithic SiC ($4.13\,s\,cm^{-2}$). These results were explained in terms of the similarity in matrices (A') and the difference in microstructure (B') between the composites and monolithic SiC.

Acknowledgements

The authors wish to express their thanks to Dr. M. Shibuya of Ube Industries Ltd. for the provision of all Tyranno® SA fibres used in this work, Dr. H.T. Hintzen and Ms. A.C.A. Delsing of Eindhoven University of Technology for the measurement of thermal diffusivity (photo-flash technique), and Dr. K. Hirao and Dr. H. Hayashi of the National Institute of Advanced Industrial Science and Technology (Chubu) for the measurement of thermal diffusivity (laser-flash technique).

References

1. Schlichting, J. and Riley, F. L., In *Concise Encyclopedia of Advanced Ceramic Materials*, ed. R. J. Brook. Pergamon Press, Oxford, 1991, pp. 426–429.
2. Ishikawa, T., Yamamura, Y., Hirokawa, T., Hayashi, Y., Noguchi, Y. and Matsushima, M., Strength and fracture toughness properties of oxidation resistant high-temperature ceramic matrix composites. In *Proceedings of the Ninth International Conference on Composite Materials*, ed. A. Miravette. Woodhead Publishing Co., Cambridge, UK, 1993, pp. 137–144.
3. Davies, I. J., Ishikawa, T., Shibuya, M., Hirokawa, T. and Gotoh, J., Fibre and interfacial properties measured in situ for a 3-D woven SiC/SiC-based composite with glass sealant. *Composites Part A*, 1999, **30**, 587–591.
4. Kmetz, M. and Suib, S., Silicon carbide/silicon and silicon carbide/silicon carbide composites produced by chemical vapor infiltration. *J. Am. Ceram. Soc.*, 1990, **73**, 3091–3093.
5. Kagawa, Y. and Goto, K., Notch sensitivity of two-dimensional woven SiC fibre-reinforced SiC matrix composite fabricated by the polymer conversion process. *J. Mater. Sci. Lett.*, 1997, **16**, 850–854.
6. Itatani, K., Hattori, K., Harima, D., Aizawa, M., Okada, I., Davies, I. J., Suemasu, H. and Nozue, A., Mechanical and thermal properties of silicon-carbide composites fabricated with short Tyranno® Si—Zr—C—O fibre. *J. Mater. Sci.*, 2001, **36**, 3679–3686.
7. Lee, J.-S., Yoshida, K. and Yano, T., Influence of fiber volume fraction on the mechanical and thermal properties of unidirectionally aligned short fiber reinforced SiC composites. *J. Ceram. Soc. Jpn.*, 2002, **110**, 985–989.
8. Lee, J.-S. and Yano, T., Fabrication of short-fiber-reinforced SiC composites by polycarbosilane infiltration. *J. Eur. Ceram. Soc.*, 2004, **24**, 25–31.

9. Itatani, K. and Davies, I. J., Mechanical properties of silicon carbide composites fabricated with short inorganic fibers. *Recent Res. Dev. Maters. Sci.*, 2002, **3**, 427–439.
10. Yamamura, T., Ishikawa, T., Shibuya, M., Hisayuki, T. and Okamura, K., Development of a new continuous Si─Ti─C─O fiber using an organometallic polymer precursor. *J. Mater. Sci.*, 1988, **23**, 2589–2594.
11. Ishikawa, T., Kohtoko, Y., Kumagawa, K., Yamamura, T. and Nagasawa, T., High-strength alkali-resistant sintered SiC fibre stable to 2200 °C. *Nature*, 1998, **391**, 773–775.
12. Itatani, K., Tanaka, T., Suemasu, H., Nozue, A. and Davies, I. J., Fabrication and fracture behaviour of silicon carbide composites containing chopped Tyranno® Si─Al─C fibre. *J. Aust. Ceram. Soc.*, 2005, **41**, 1–7.
13. Sato, M., Itatani, K., Tanaka, T., Davies, I. J., and Koda, S., Effect of chopped Si─Al─C fiber addition on the mechanical properties of silicon carbide composites, *J. Mater. Sci.*, submitted for publication.
14. Nieto, M. I., Martínez, R., Mazerolles, L. and Baudín, C., Improvement in the thermal shock resistance of alumina through the addition of submicron-sized aluminium nitride particles. *J. Eur. Ceram. Soc.*, 2004, **24**, 2293–2301.
15. Slack, G. A., Nonmetallic crystals with high thermal conductivity. *J. Phys. Chem. Solids*, 1973, **34**, 321–335.
16. Takeda, Y., Development of high-thermal-conductive SiC ceramics. *Am. Ceram. Soc. Bull.*, 1988, **67**, 1961–1963.
17. Giancarli, L., Bonal, J. P., Caso, A., Le Marois, G., Morley, N. B. and Salavy, J. F., Design requirements for SiC/SiC composites structural material in fusion power reactor blankets. *Fusion End. Des.*, 1998, **41**, 165–171.
18. Kowbel, W., Bruce, C. A., Tsou, K. L., Patel, K., Withers, J. C. and Youngblood, G. E., High thermal conductivity SiC/SiC composites for fusion applications. *J. Nucl. Mater.*, 2000, **283–287**, 570–573.
19. Yoshida, K., Imai, M. and Yano, T., Room- and high-temperature thermal conductivity of silicon carbide fiber-reinforced silicon carbide composites with oxide sintering additives. *J. Ceram. Soc. Jpn.*, 2001, **109**, 863–867.
20. Youngblood, G. E., Senor, D. J. and Jones, R. H., Modeling the transverse thermal conductivity of 2D-SiC_f/SiC composites. *Fusion Mater.*, 2001, **31**, 57–63.
21. Katoh, Y., Kohyama, A., Nozawa, T. and Sato, M., SiC/SiC composites through transient eutectic-phase route for fusion applications. *J. Nucl. Mater.*, 2004, **329-333**, 587–591.
22. Yamada, R., Igawa, N. and Taguchi, T., Thermal diffusivity/conductivity of Tyranno SA fiber and Hi-Nicalon Type S fiber-reinforced 3-D SiC/SiC composites. *J. Nucl. Mater.*, 2004, **329–333**, 497–501.
23. Collin, M. I. K. and Rowcliffe, D. J., Influence of thermal conductivity and fracture toughness on the thermal shock resistance of alumina–silicon–carbide–whisker composites. *J. Am. Ceram. Soc.*, 2001, **84**, 1334–1340.
24. Graham, S. and McDowell, D. L., Numerical analysis of the transverse thermal conductivity of composites with imperfect interfaces. *J. Heat Transfer*, 2003, **125**, 389–393.
25. Hasselman, D. P. H., Effect of cracks on thermal conductivity. *J. Compos. Mater.*, 1978, **12**, 403–407.
26. Berbon, M. Z., Dietrich, D. R., Marshall, D. B. and Hasselman, D. P. H., Transverse thermal conductivity of thin C/SiC composites fabricated by slurry infiltration and pyrolysis. *J. Am. Ceram. Soc.*, 2001, **84**, 2229–2234.
27. Kingery, W. D., Howen, H. K. and Uhlmann, D. R., *Introduction to Ceramics* (*2nd ed.*). John Wiley and Sons, New York, 1976, pp. 583–645.
28. Eucken, A., Thermal conductivity of ceramic refractory materials: calculation from thermal conductivities of constituents. *Forsch. Gebiete Ingenieurw.*, 1932, **B3**(353), 16.
29. Russell, L. M., Johnson, L. F., Hasselman, D. P. H. and Ruh, R., Thermal conductivity/diffusivity of silicon carbide whisker reinforced mullite. *J. Am. Ceram. Soc.*, 1987, **70**, C-226–C-229.
30. Luo, J., Stevens, R. and Taylor, R., Thermal diffusivity/conductivity of magnesium oxide/silicon carbide composites. *J. Am. Ceram. Soc.*, 1997, **80**, 699–704.
31. Barea, R., Belmonte, M., Osendi, M. I. and Miranzo, P., Thermal conductivity of Al_2O_3/SiC platelet composites. *J. Eur. Ceram. Soc.*, 2003, **23**, 1773–1778.
32. Berman, R., *Thermal Conduction in Solids*. Claredon Press, Oxford, UK, 1976.
33. Munro, R. G., Material properties of a sintered alpha-SiC. *J. Phys. Chem. Ref. Data*, 1997, **26**, 1195–1203.
34. Kumagawa, K., Yamaoka, H., Shibuya, M. and Yamamura, T., Fabrication and mechanical properties of new improved Si─M─C─(O) Tyranno® fiber. *Ceram. Eng. Sci. Proc.*, 1998, **19**, 65–72.
35. German, R. M., Hens, K. F. and Johnson, J. L., Powder metallurgy processing of thermal management materials for microelectronic applications. *Int. J. Powder Metall.*, 1994, **30**, 205–214.
36. Suemitsu, T., Takashima, A. and Nishikawa, H., Improvement of oxidation resistance of carbon/carbon composites by the multi-layer CVD coating technique. *J. Ceram. Soc. Jpn.*, 1995, **103**, 479–483.
37. Powers, J. M. and Somorjai, G. A., The surface oxidation of alpha-silicon carbide by O_2 from 300 to 1373 K. *Surf. Sci.*, 1991, **244**, 39–50.
38. Zhang, Y. and Binner, J., In situ surface modification of silicon carbide particles using Al^{3+} complexes and polyelectrolytes in aqueous suspensions. *J. Am. Ceram. Soc.*, 2002, **85**, 529–534.
39. Raffray, A. R., El-Guebaly, L., Sze, D. K., Billone, M., Sviatoslavsky, I., Mogahed, E., Najmabadi, F., Tillack, M. S., and Wang, X., SiC/SiC composite for an advanced fusion power plant blanket, In *Proceedings of the 18th IEEE/NPSS Symposium of Fusion Engineering*. Albuquerque, NM, October 1999, pp. 73–76.
40. Nakayasu, T., Sato, M., Yamamura, T., Okamura, K., Katoh, Y. and Kohyama, A., Recent advancement of Tyranno/SiC composites R&D. *Ceram. Eng. Sci. Proc.*, 1999, **20**, 301–308.
41. Garboczi, E. J., Snyder, K. A., Douglas, J. F. and Thorpe, M. F., Geometrical percolation threshold of overlapping ellipsoids. *Phys. Rev.*, 1995, **E52**, 819–828.
42. Hasselman, D. P. H. and Johnson, L. F., Effective thermal conductivity of composites with interfacial thermal barrier resistance. *J. Compos. Mater.*, 1987, **21**, 508–515.
43. Youngblood, G. E., Senor, D. J., Jones, R. H. and Graham, S., The transverse thermal conductivity of 2D-SiCf/SiC composites. *Compos. Sci. Technol.*, 2002, **62**, 1127–1139.
44. Debye, P., Equation of state and quantum hypothesis for thermal conductivity with an appendix (Zustandsgleichung und qantenhypotheses mit einem anhang über wärmeleitung), In *Lectures on the kinetic theory of materials and electricity* (Vorträge über die Kinetische Theorie der Materie und der Elektizität). Teubner, Berlin, 1914, pp. 19–60.
45. Bruls, R. J., Ph.D. thesis, The thermal conductivity of magnesium silicon nitride, $MgSiN_2$, ceramics and related materials. Eindhoven University of Technology, 2000, pp. 203–235.
46. Bruls, R. J., Hintzen, H. T. and Metselaar, R., A new estimation method for the intrinsic thermal conductivity of non-metallic compounds. A case study for $MgSiN_2$, AlN, and β-Si_3N_4 ceramics. *J. Eur. Ceram. Soc.*, 2005, **25**, 767–779.
47. Roufosse, M. and Klemens, P. G., Thermal conductivity of complex dielectric crystals. *Phys. Rev. B*, 1973, **7**, 5379–5386.
48. Joshi, R. P., Neudeck, P. G. and Fazi, C., Analysis of the temperature dependent thermal conductivity of silicon carbide for high temperature applications. *J. Appl. Phys.*, 2000, **88**, 265–269.
49. Iwata, H., Lindefelt, U., Oberg, S. and Briddon, P. R., Localized electronic states around stacking faults in silicon carbide. *Phys. Rev. B*, 2001, **65**, 33203–33206.